GENERALISED TENSION-STIFFENING RELATIONSHIP CONFORMING TO CHINESE DESIGN CODE GB 50010-2010

Gintaris Kaklauskas [1,*], Viktor Gribniak [1,2], P.L. Ng [1,3], Eugenijus Gudonis [1,2] and Ronaldas Jakubovskis [1]
[1] Department of Bridges and Special Structures, Vilnius Gediminas Technical University, Sauletekio al. 11, LT-10223 Vilnius, Lithuania. *Email: Gintaris.Kaklauskas@vgtu.lt
[2] Research Laboratory of Innovative Building Structures, Vilnius Gediminas Technical University, Sauletekio al. 11, LT-10223 Vilnius, Lithuania.
[3] Department of Civil Engineering, The University of Hong Kong, Pokfulam, Hong Kong, China.

ABSTRACT

A generalised stress-strain tension-stiffening relationship conforming to the Chinese Code for Design of Concrete Structures GB 50010-2010 is proposed. Based on the provisions in GB 50010-2010 for rigidity and curvature calculations of reinforced concrete flexural members, tension-stiffening relationships were derived from moment-curvature relations by means of the inverse technique for deformation analysis. A parameterized stress block for tension-stiffening was suggested. The proposed tension-stiffening model was applied to nonlinear finite element analysis of reinforced concrete beams. Good agreement between the analysis results based on the proposed model and those based on the codified formulas in GB 50010-2010 was achieved. The proposed model will be able to serve as a design aid for serviceability evaluation of concrete beams in general.

KEYWORDS

Chinese code, moment-curvature relation, reinforced concrete design, tensile stress block, tension-stiffening.

INTRODUCTION

In reinforced concrete design practice, deformation and cracking control are key aspects in serviceability limit state (SLS) so as to ensure the stiffness, integrity, human comfort, durability, and aesthetics of the structures. The Chinese Code for Design of Concrete Structures GB 50010-2010 (MOHURD 2010) stipulates requirements in satisfying the SLS of structures, and the code contains provisions for crack width calculation and deflection checking. When conducting checking against SLS in structural design, the load combinations for SLS shall be composed, where the load factors should be determined in accordance with the requirements in the Load Code for the Design of Building Structures GB 50009-2012 (MOHURD 2012) based on the functional use of structure, the type of loading, the persistency of loading, and relevant site-specific conditions. Pertaining to the load combination, the structural actions should be determined, and checking of crack width and deflection should be performed.

A limitation with the use of codified formulations is that their range of applications is confined to relatively regular structures. For the design of irregular or complex structures, the formulations might not be directly applicable, and alternative methodology such as the use of sophisticated numerical techniques would be necessary. With the advent of high-strength concrete and high-performance concrete, long-span concrete structures have been gaining increasing popularity. The serviceability criterion of long-span members is often the governing condition of the design, and deflection control of concrete flexural members has become a critical issue under the SLS. However, the load-deflection response of cracked concrete members is not straightforward. After cracking, the intact concrete between cracks can transfer tensile forces normal to the crack plane to the reinforcement through the bond, which contributes to the overall stiffness of the member. This is referred to as the tension-stiffening phenomenon (Gilbert 2008; Ng *et al*. 2010). Researches have confirmed that the deflection behaviour of cracked beams is significantly influenced by the tension-stiffening effect (Kaklauskas 2001; Torres *et al*. 2004; Khalfallah 2008; Lam *et al*. 2010), which should be duly considered in the SLS checking.

Herein, the authors derive a generalised stress-strain tension-stiffening relationship conforming to the provisions in GB 50010-2010. The model will enable deflection checking in the design stage by simple numerical methods, and the deflection checking would deem to satisfy the codified requirements. The inverse technique for deformation analysis developed by Kaklauskas and Ghaboussi (2001) and subsequently modified by Gribniak (2009) and Kaklauskas and Gribniak (2011) is employed for derivation of tension-stiffening relationships from the moment-curvature diagrams calculated based on GB 50010-2010 formulations. To confirm the applicability

of the proposed model, it is adopted in structural analysis of concrete beams with the use of the nonlinear finite element software ATENA. It is envisaged that the proposed model would serve as a design aid for assessing the serviceability performance of concrete beams with variable structural configurations.

RELEVANT PROVISIONS IN GB 50010-2010

In this section, the provisions in GB 50010-2010 (mainly from Clauses 7.2.3 and 7.2.4) in relation to rigidity calculation and curvature analysis for reinforced concrete flexural members are extracted and elaborated. The notations used are basically following the definitions in GB 50010-2010, unless otherwise stated. The short-term curvature κ is related to the applied bending moment and rigidity, as described by the following equation:

$$\kappa = \begin{cases} M_{ext}/B_{s1}, \text{if } M_{ext} < M_{cr} \\ M_{ext}/B_{s2}, \text{if } M_{ext} \geq M_{cr} \end{cases} \quad (1)$$

where M_{ext} and M_{cr} are respectively the external bending moment and the cracking moment, B_{s1} and B_{s2} are respectively the rigidity of uncracked and cracked sections, and are calculated by the following equations:

$$B_{s1} = E_c I_0 \quad (2)$$

$$B_{s2} = \frac{E_s A_s h_0^2}{1.15\psi + 0.2 + 6\alpha_E \rho / \left(1 + 3.5\gamma_f'\right)} \quad (3)$$

in which E_c is the elastic modulus of concrete, I_0 is the moment of inertia of the transformed section, E_s is the elastic modulus of reinforcing steel, A_s is the tension reinforcement area, h_0 is the effective depth of section, ρ is the tension reinforcement ratio ($\rho = A_s/bh_0$, where b denotes the breadth of section), α_E is the modular ratio of reinforcement and concrete ($\alpha_E = E_s/E_c$), γ_f' is the ratio of sectional area of compression flange to effective sectional area of web, and ψ is a coefficient to account for the non-uniformity of strain in tension reinforcement between cracks, and is defined by the following equation:

$$\psi = 1.1 - 0.65\frac{f_{ct}}{\rho_{te}\sigma_s}, \left(0.2 \leq \psi \leq 1.0\right) \quad (4)$$

In Equation (4), f_{ct} is the characteristic tensile strength of concrete, ρ_{te} denotes the quotient of A_s divided by the area of tension zone of concrete section, and σ_s is the stress in tension reinforcement.

The cracking moment M_{cr} in Equation (2) is determined as:

$$M_{cr} = \gamma f_{ct} W_0 \quad (5)$$

where W_0 is the elastic sectional modulus with respect to the extreme tension fibre of the transformed section, γ is the plastic influence coefficient for sectional resisting moment of concrete member and is defined by:

$$\gamma = \left(0.7 + \frac{120}{h}\right)\gamma_m \quad (6)$$

In Equation (6), h is the depth of section in mm and γ_m is the basic value of the plastic influence coefficient and has a value of 1.55 for rectangular sections.

INVERSE TECHNIQUE FOR DEFORMATION ANALYSIS

The inverse technique is used for computing the stress-strain tension-stiffening relationship under the equilibrium conditions of forces and bending moments, from a given moment-curvature or moment-deflection diagram (Kaklauskas and Ghaboussi 2001). It employs an iterative procedure of deformation analysis based on the layer section model (Kaklauskas 2004). The following basic assumptions are involved: (1) smeared crack approach, (2) linearity and continuity of strain distribution within the depth of section - this implies perfect bond between layers; and (3) concrete layers in the tension zone follow an uniform stress-strain tension-stiffening law. These assumptions are rational with respect to the structural behaviour of reinforced concrete beams.

To illustrate the inverse analysis, first consider the solution of structural response of a doubly reinforced concrete member subjected to pure bending by the direct analysis. Figure 1(a) depicts the cross-section of the member, which is divided into horizontal layers corresponding to either concrete or reinforcement (Figure 1(b)). The thickness of reinforcement layer is determined from the condition of equivalent steel area. Denote the external bending moment by M_{ext}, based on the principal of equilibrium and from the material diagrams (which will be further discussed in the below), equilibrium equations can be set up with respect to Figure 1(c). By solving the equilibrium equations, the level of neutral axis and the concrete stress at extreme fibres can be obtained. As the extreme fibre has the maximum strain, by proportionality and from the curvature κ, the strain ε_i at any layer i (refer to Figure 1(d)) can be calculated by means of Equation (7). For the given strain ε_i at any

layer i, by substituting known values into the equilibrium equations, the stress at the layer σ_i is obtained. The stress distribution within the layer section model can be computed and is schematically presented in Figure 1(e).

$$\kappa = \frac{M_{ext}}{IE}; \quad \varepsilon_i = \kappa(y_i - y_c); \quad y_c = \frac{SE}{AE}; \quad AE = \sum_{i=1}^{n} b_i t_i E_{i,\sec}$$
$$SE = \sum_{i=1}^{n} b_i t_i y_i E_{i,\sec}; \quad IE = \sum_{i=1}^{n} \left[\frac{t_i^2}{12} + (y_i - y_c)^2 \right] b_i t_i E_{i,\sec} \tag{7}$$

In the above, AE, SE and IE are the area, the first and the second moments of the area multiplied by secant deformation modulus $E_{i,sec}$, n is the total number of layers, b_i and t_i are respectively the width and thickness of the i-th layer (for a beam with rectangular cross-section, b_i is a constant), y_i is the distance of the i-th layer from the top edge of section, and y_c is the distance of neutral axis from the top edge of section. The notations of other symbols may refer to Figure 1. The materials models assumed in the analysis are illustrated diagrammatically in Figures 1(f), 1(g) and 1(h) for the reinforcement, concrete in compression and concrete in tension, respectively. It should be noted that in this study, the reinforcement is treated as ideally elastic-plastic, and the concrete in compression is modelled by adopting the stress-strain relationship per Appendix C of GB 50010-2010. For the implementation of inverse technique in this research, the material model of concrete in tension is to be determined by back-analysis of moment-curvature diagrams calculated per GB 50010-2010, instead of pre-defined by assumption. For each layer, the secant deformation modulus is determined as $E_{i,sec} = \sigma_i/\varepsilon_i$ ($i = 1 \ldots n$). The analysis is performed iteratively until convergence of secant modulus at each layer is attained. The calculation is terminated when the final loading step is reached.

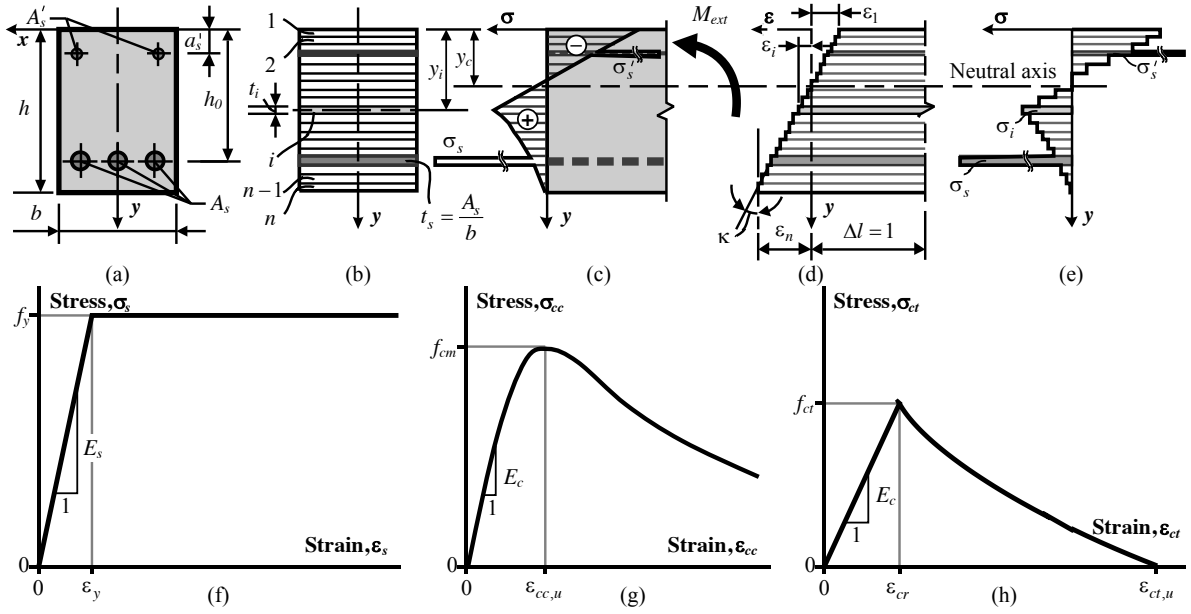

Figure 1 (a)–(e) Layer section model; (f) material diagram for reinforcement steel; (g) material diagram for concrete in compression; (h) material diagram for concrete in tension

To obtain the moment-curvature diagrams based on GB 50010-2010 provisions, the direct technique is utilised. The direct analysis allows prediction of structural response using specified constitutive model and section properties. Whereas to obtain the tension-stiffening relationship from the moment-curvature diagrams, the inverse technique is used. In contrast to direct analysis, the inverse analysis aims at determining parameters of the model based on the response of the structure. Kaklauskas and Ghaboussi (2001) formulated the principles of inverse technique for deriving the average tensile stress-strain relationship of concrete using test data of reinforced concrete beam specimens. From the experimentally-obtained moment-curvature curves, back-analysis was performed with the layer section model via load (bending moment) increments. At each step of load increment, the depth of neutral axis and the concrete stress in the extreme tension fibre were determined by solving the equilibrium equations. Since the extreme fibre has the largest strain, other tension fibres of concrete having smaller strains fall within the portion of the stress-strain diagram which had already been determined (the third assumption in the above). The average stress-strain relationship of concrete in tension was progressively derived along with the bending moment increments.

The present research employs the inverse technique which was modified by Gribniak (2009) and Kaklauskas and Gribniak (2011). The flowchart in Figure 2 illustrates the analysis procedures algorithmically. Computations are performed iteratively via bending moment increments. At each moment increment j, an initial value of secant deformation modulus of the stress-strain relationship is assumed. The curvature $\kappa_{th,j}$ is calculated by the direct analysis. If the relative error $\delta_{j,k}$ between the calculated and the target curvature per codified formulations $\kappa_{code,j}$ does not exceed the tolerance Δ, the basic convergence condition is satisfied (it should be noted that the entire convergence criteria comprise also the changes in internal forces, internal bending moments, and secant moduli of all layers are within specified allowable limits) and the analysis can proceed to the next step of moment increment with an updated secant deformation modulus of each layer. Mathematically, the comparison between relative error and tolerance is represented by the following:

$$\left|\delta_{j,k}\right| = \left|\frac{\kappa_{th,j}}{\kappa_{code,j}} - 1\right| \le \Delta \tag{8}$$

Conversely, if $|(\kappa_{th,j}/\kappa_{code,j}) - 1| > \Delta$, i.e. convergence condition is not met, the analysis is repeated with the secant modulus adjusted by the hybrid Newton-Raphson and bisection procedure (Gribniak 2009; Gribniak *et al*. 2012) until convergence is attained or the iteration number reaches its limit N, which is set at 100 or other values to suit the numerical procedures. Then the analysis proceeds to the next increment step until the final loading step is reached. As of the Newton-Raphson method, it is for root finding of the secant deformation modulus. For brevity, denote the modulus at moment increment j and iteration k by short-hand $E_{j,k}$, and the modulus at moment increment j and iteration (k–1) by short-hand $E_{j,k\text{-}1}$. The updating of modulus is defined by:

$$E_{j,k} = E_{j,k-1} - \frac{\delta\left(E_{j,k-1}\right)}{\delta'\left(E_{j,k-1}\right)} \tag{9}$$

where $\delta'(E_{j,k\text{-}1})$ is the first derivative of the relative error numerically obtained from the central difference equation:

$$\delta'(E) = \frac{-\delta_{II} + 8\delta_{I} - 8\delta_{-I} + \delta_{-II}}{12\eta} \tag{10}$$

$$\delta_{II} = \delta(E+2\eta); \quad \delta_{I} = \delta(E+\eta); \quad \delta_{-I} = \delta(E-\eta); \quad \delta_{-II} = \delta(E-2\eta) \tag{11}$$

with η being the step of difference grid in the Newton-Raphson procedure, and the symbols δ_{II}, δ_{I}, δ_{-I} and δ_{-II} are evaluated per Equation (11). It is noted that in these equations, the indices of the secant deformation modulus are omitted.

During the numerical implementation, if the root found by the Newton-Raphson method does lead to an admissible solution, the updated modulus is used for further analysis. However, if the root is localised and does not lead to an admissible solution, i.e. $\delta(E_{j,k})\cdot\delta(E_{j,k\text{-}1}) < 0$, the analysis would proceed using the bisection method, which reduces the root localisation interval $[E_1, E_2]$ each time until it becomes sufficiently small. The updating of modulus is described by the following:

$$E_{j,k+1} = E_1 + 0.5(E_2 - E_1) \tag{12}$$

$$[E_1, E_2] = \begin{cases} [E_1, E_{j,k}], \text{ if } \delta(E_1)\delta(E_{j,k}) \le 0 \\ [E_{j,k}, E_2], \text{ if } \delta(E_1)\delta(E_{j,k}) > 0 \end{cases} \tag{13}$$

Unlike the Newton-Raphson method, the bisection method requires a single evaluation of $\delta(E)$ per iteration. Through the above numerical process, it yields the average stress-strain tension-stiffening relationship.

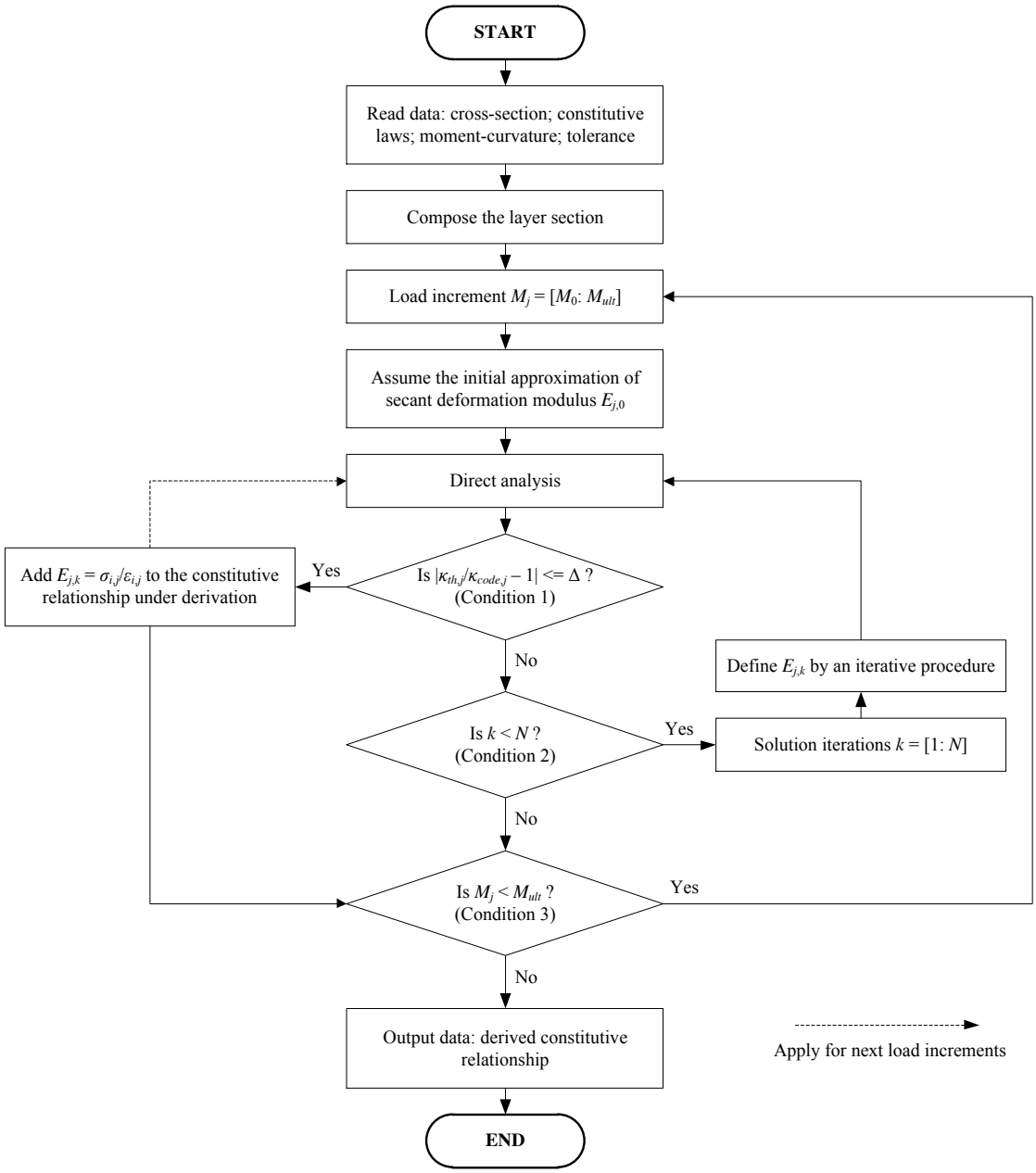

Figure 2 Flowchart of inverse technique

DERIVATION OF TENSION-STIFFENING RELATIONSHIP

The relationship between tension-stiffening behaviour and moment-curvature response is illustrated in Figure 3(a). Consider a simply-supported beam subjected to an increasing loading. When the moment is less than the cracking moment M_{cr}, the beam is uncracked and the response is described by the line segment OA. Upon reaching the cracking moment, the beam is cracked and its stiffness reduces instantly. And the actual moment-curvature response would be along the line segment AB. While assuming the concrete does not carry tension, its moment-curvature response would be along the line segment OC. The difference between OAB and OC represents the stiffening effect by concrete in resisting tension. Further consider the load at service, under which the curvature would be represented by the abscissa of intersection between the level of service bending moment M_{ser} and the moment-curvature curve. It can be seen that the level of M_{ser} insects OAB and OC at different abscissas, indicating that the beam curvature and deflection would be overestimated by neglecting the effect of tension-stiffening.

In deriving the generalised tension-stiffening relationship, the methodology as detailed in the preceding paragraphs is employed. As a numerical experiment, the moment-curvature diagrams of 360 nos. reinforced

concrete beams are calculated per GB 50010-2010. Uniform rectangular cross-section of 200 mm by 400 mm was considered. The concrete grade was varied from C40 to C75. The reinforcement ratio ρ was varied from 0.25% to 2.25%, the modulus of elasticity of reinforcing steel E_s was fixed at 200 GPa per GB 50010-2010 stipulations, the modular ratio α_E was varied from 5.33 to 6.14, and the effective depth to overall section depth ratio h_0/h was varied from 0.725 to 0.925. Figure 3(b) depicts the typical cross-section of the beams.

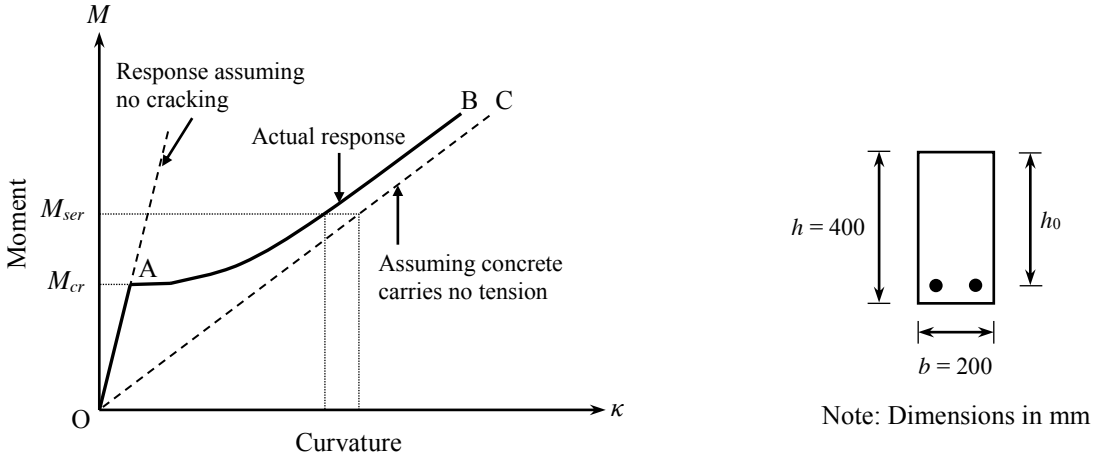

Figure 3 Typical moment-curvature diagram and cross-section of beams

In the layer section model, the cross-section was divided into 200 layers. The centreline of reinforcement layer was coinciding with the centres of reinforcing bars, and the thickness of reinforcement layer t_s was computed as $t_s = A_s/b$. The remaining height portions of the cross-section above and below the reinforcement layer were equally and separately divided into the concrete layers. The number of concrete layers above the reinforcement layer was taken as the nearest integer value of $(n–1)(h_0–t_s/2)/(h–t_s)$, whereas the number of concrete layer below the reinforcement layer was taken as the nearest integer value of $(n–1)(h–h_0–t_s/2)/(h–t_s)$. And the thickness of layers within each height portion was computed with respect to the number of layers and the height of portion.

Through the analysis, the moment-curvature diagram for each beam was obtained by using the procedures outlined in Figure 2. The ultimate bending moment was divided into approximately 90 increment steps. Generally, the step sizes were coarser prior to cracking, and were finer once the cracking moment is reached. Such arrangement is to accord with the basically linear behaviour of tensile stress-strain relation before cracking and its nonlinearity after cracking.

For each moment-curvature diagram, a tension-stiffening relationship was computed by the aforementioned inverse technique. Examples of tension-stiffening relationships are presented in Figure 4 for illustration. From the tension-stiffening diagrams, it can be seen that the stress increases with the strain from the origin up to the maximum value of tensile stress, and drops abruptly to around 40% to 65% of the maximum value, and thereafter gradually decreases with increasing strain. Such abrupt drop in tensile stress was also reported in Damjanic and Owen (1984), Kaklauskas and Ghaboussi (2001), and Kwan *et al*. (2008). As all the tension-stiffening diagrams have similar geometrical characteristics in common, a generalised stress block conforming to GB 50010-2010 can be developed. For ease of implementation, a simple parameterized stress block is proposed herein to simulate the average stress-strain behaviour of tensile concrete. The stress block is depicted in Figure 5. Prior to cracking, the stress block is assumed to be ascending in a linearly elastic manner. The maximum stress γf_{ct} is reached at strain $\gamma\varepsilon_{cr}$, where the stress drops abruptly to αf_{ct}, and linearly and gradually descends to zero at strain $\beta\varepsilon_{cr}$. The abrupt drop of stress is controlled by the parameter α, and the descending branch is controlled by parameters α and β. The following formulation is proposed for the generalised tension-stiffening model:

$$\sigma = \begin{cases} E_c\varepsilon, \text{ if } \varepsilon \le \gamma\varepsilon_{cr} \\ \dfrac{\alpha f_{ct}(\beta\varepsilon_{cr} - \varepsilon)}{\beta\varepsilon_{cr} - \gamma\varepsilon_{cr}}, \text{ if } \gamma\varepsilon_{cr} < \varepsilon \le \beta\varepsilon_{cr} \\ 0, \text{ if } \beta\varepsilon_{cr} < \varepsilon \end{cases} \tag{14}$$

where

$$\alpha = \frac{\sigma}{f_{ct}} \tag{15}$$

$$\beta = \frac{\varepsilon}{\varepsilon_{cr}} \tag{16}$$

In the equations above, γ is as defined in GB 50010-2010, $\varepsilon_{cr} = f_{ct}/E_c$ is the cracking strain. The proposed model is can be easily programmed or input in structural analysis software for automation in design.

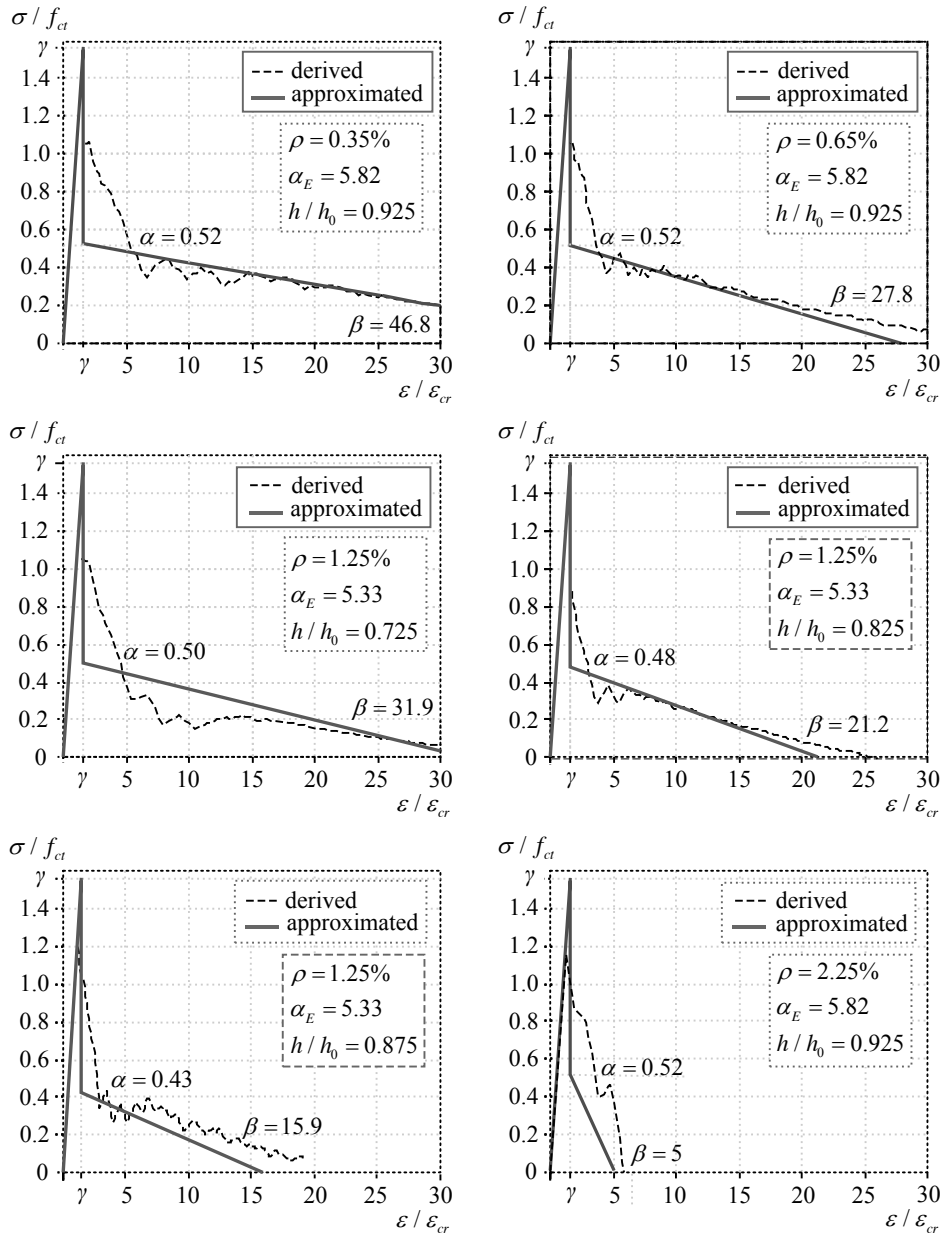

Figure 4 Derived and approximated tension-stiffening relationships

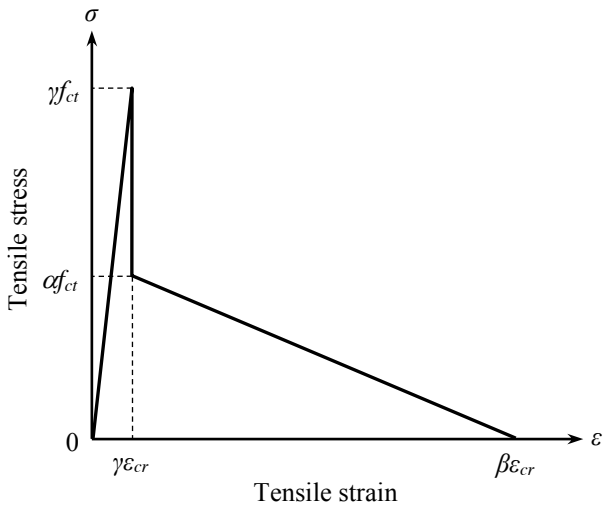

Figure 5 Proposed tension-stiffening model

The proposed tension-stiffening model was established from and validated by numerical experiment consisting of a large number of reinforced concrete beams with varying concrete grades, tension reinforcement ratios, modular ratios of reinforcement to concrete, and effective depth to overall depth ratios. Among these variables, the tension reinforcement ratio was found to have more influence on the shape of stress block, particularly on the value of β. The dependence of the tension-stiffening relationship on the tension reinforcement ratio can be observed from Figure 4. Further numerical studies are ongoing in order to develop accurate and reliable formulas for the parameters α and β applicable for a wide range of concrete beam configurations, as well as to assess the plausible numerical deviations by statistical means. This part of research will be reported in due course.

APPLICATION TO FINITE ELEMENT ANALYSIS

To illustrate the applicability of the proposed tension-stiffening model, it was incorporated into the nonlinear finite element software ATENA for analysis of reinforced concrete beams. The beams have uniform cross-section of 200 mm in width and 400 mm in depth, subjected to two-point loading applied in a symmetrical manner. The distance between loading points is 1.0 m, the shear span at each side is 1.0 m, and the distance between a support point and the beam end is 0.14 m. The total length of beam is 3.28 m. Perfect bond between concrete and steel reinforcement was assumed. To avoid stress concentrations, steel plates of 80 mm in breadth and 30 mm in thickness were mounted to the beam at the loading points and support points. The finite element model is shown in Figure 6. Quadrilateral plane stress finite elements were employed with the use of 50 mm mesh size and 100 mm characteristic length. The ultimate load was divided approximately into 50 increment steps. Standard Newton-Raphson method was used in performing iterations.

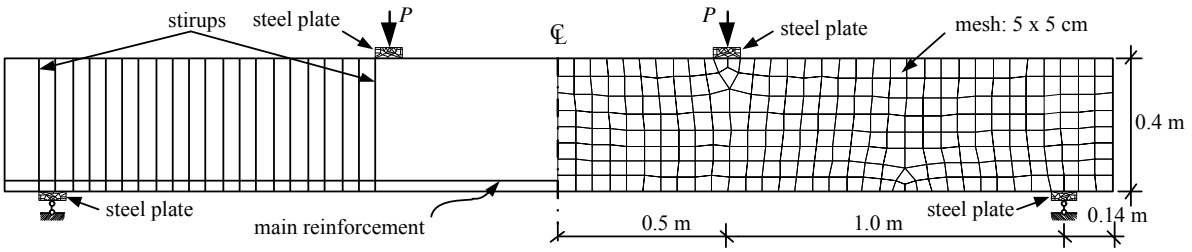

Figure 6 Finite element model in ATENA

The beams are cast from grade C45 concrete. The tension reinforcement ratios, modular ratios, and effective depth to overall depth ratios of beams are shown in Figure 7, which depicts the comparison the moment-curvature diagrams calculated per GB 50010-2010 and the results from ATENA incorporating the proposed model. Good agreement between GB 50010-2010 and ATENA results can be observed. The curvature predictions at the service load level are compared. In practice, the bending moment at service load is usually in the range of 40% to 60% of the ultimate bending moment. Herein, the value of M_{ser} is taken as $0.55M_{ult}$. It is found that the errors of curvature predictions corresponding to the service bending moment were well below 5%.

Though concrete beams with rectangular cross-section are presented herein, beams with variable sections and structural configurations can be analysed by finite element method using the same tension-stiffening model for serviceability checking.

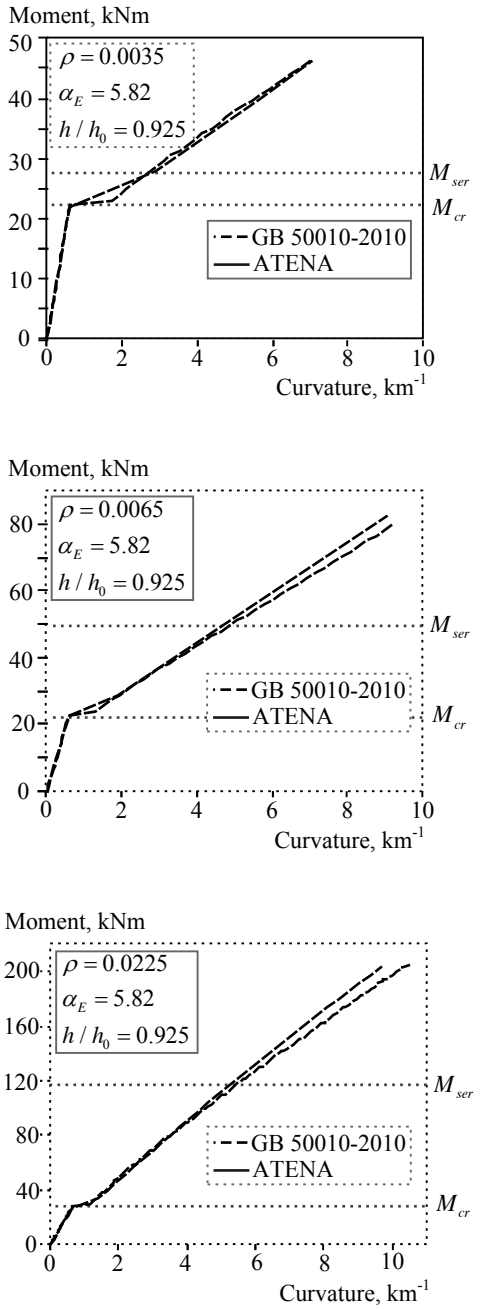

Figure 7 Analytical moment-curvature curves

CONCLUSIONS

In this paper, the authors have proposed a generalised tension-stiffening law conforming to the provisions in the Chinese design code GB 50010-2010 for deformation analysis of reinforced concrete flexural members. By applying the inverse technique developed in precedence, the tension-stiffening relationships have been derived based on the moment-curvature diagrams calculated per GB 50010-2010. A parameterized stress block with simple formulation to account for the tension-stiffening effect has been proposed. The proposed tension-stiffening model has been incorporated in nonlinear finite element analysis of concrete beams to confirm its applicability. From the results of studies, it is concluded that the proposed model can be applied to deformational analysis of reinforced concrete flexural members for serviceability evaluation.

ACKNOWLEDGMENT

The authors gratefully acknowledge the financial support provided by the Research Council of Lithuania (Project No. MIP-050/2014).

REFERENCES

Damjanic, F. and Owen, D.R.J. (1984). "Practical considerations for modelling of post-cracking concrete behaviour for finite-element analysis of reinforced concrete structures", In F. Damjanic, E. Hinton, N. Bicanic and V. Simovic, eds. *Proceedings, International Conference on Computer Aided Analysis and Design of Concrete Structures*, Split, Yugoslavia, 693-706.

Gilbert, R.I. (2008). "Revisiting the tension stiffening effect in reinforced concrete slabs". *Australian Journal of Structural Engineering*, 8(3), 189-196.

Gribniak, V. (2009). *Shrinkage Influence on Tension-Stiffening of Concrete Structures*, PhD Thesis, Vilnius Gediminas Technical University, Vilnius, Lithuania, 191.

Gribniak, V., Kaklauskas, G., Kacianauskas, R. and Kliukas, R. (2012). "Improving efficiency of inverse constitutive analysis of reinforced concrete flexural members". *Scientific Research and Essays*, 7(8), 923-938.

Kaklauskas, G. (2001). *Integral Flexural Constitutive Model for Deformational Analysis of Concrete Structures*, Vilnius Gediminas Technical University, Vilnius: Technika, Lithuania, 139.

Kaklauskas, G. and Ghaboussi, J. (2001). "Stress-strain relations for cracked tensile concrete from RC beam tests". *Journal of Structural Engineering*, ASCE, 127(1), 64-73.

Kaklauskas, G. (2004). "Flexural layered deformational model of reinforced concrete members". *Magazine of Concrete Research*, 56(10), 575-584.

Kaklauskas, G., Gribniak, V. and Bacinskas, D. (2011). "Inverse technique for deformational analysis of concrete beams with ordinary reinforcement and steel fibers". *Procedia Engineering*, 14, 1439-1446.

Kaklauskas, G. and Gribniak, V. (2011). "Eliminating shrinkage effect from moment-curvature and tension-stiffening relationships of reinforced concrete members". *Journal of Structural Engineering*, ASCE, 137(12), 1460-1469.

Khalfallah, S. (2008). "Tension stiffening bond modeling of cracked flexural reinforced concrete beams". *Journal of Civil Engineering Management*, 14(2), 131-137.

Kwan, A.K.H., Lam, J.Y.K. and Ng, P.L. (2008). "Tension stiffening in reinforced concrete beams: a new tensile stress block", In C.K. Choi, ed. *The Proceedings of 4th International Conference on Advances in Structural Engineering and Mechanics*, Jeju, Korea, 2357-2368.

Lam, J.Y.K., Ng, P.L. and Kwan, A.K.H. (2010). "Tension stiffening in reinforced concrete beams. part 2: section and member analysis". *Proceedings of the Institution of Civil Engineers*, *Structures and Buildings*, 163(1), 29-39.

MOHURD (Ministry of Housing and Urban-Rural Development of the People's Republic of China). (2010). *GB 50010-2010: Code for Design of Concrete Structures*, China Architecture & Building Press, Beijing, China.

MOHURD (Ministry of Housing and Urban-Rural Development of the People's Republic of China). (2012). *GB 50009-2012: Load Code for the Design of Building Structures*, China Architecture & Building Press, Beijing, China.

Ng, P.L., Lam, J.Y.K. and Kwan, A.K.H. (2010). "Tension stiffening in reinforced concrete beams. part 1: FE analysis". *Proceedings of the Institution of Civil Engineers*, *Structures and Buildings*, 163(1), 19-28.

Torres, L., Lopez-Almansa F. and Bozzo, L.M. (2004). "Tension-stiffening model of cracked flexural concrete members". *Journal of Structural Engineering*, ASCE, 130(8), 1242-1251.